Chemistry Research Journal, 2021, 6(3):117-131

Available online www.chemrj.org

Research Article

ISSN: 2455-8990
CODEN(USA): CRJHA5

Solid State Study for Barbituric Acid and Uracil Thorium Complexes

M. S. Masoud[1]*, H. M. Kamel[2], M. H. Al-Saify[3]

[1]Chemistry Department, Faculty of Science, Alexandria University, Alexandria, Egypt
[2]Medical Laboratory Technology Department, Faculty of Allied Medical Sciences, Pharos University, Alexandria, Egypt
[3]Sidi Kerir Petrochemicals Company, Alexandria, Egypt

Abstract Syntheses of barbituric acid and uracil Th complexes have been reported. Elemental analysis of the prepared metal complexes, structural investigation of the complexes to know their geometries and mode of bonding based on: Infrared, electronic spectra, dielectric measurements and magnetic susceptibility were studied. The thermal behavior of $Th(BA)_2$ complex has been studied applying differential scanning calorimetry (DSC). Thermodynamic parameters, decompositions and thermal stabilities are calculated and explained. Some theoretical studies were carried out to obtain the charges, bond lengths, bond angles, and dihedral angles of the studied ligands, where the chemical potential, electronegativity, hardness and softness are determined, using hyperchem program. Molecular modeling of the ligands was performed using PC computer to give extra spot lights on the bonding properties of these compounds.

Keywords Barbituric acid and uracil Th complexes, Thermal behavior, DSC, Dielectric measurements, Molecular Modeling

*Corresponding Author E-mail: drmsmasoud@yahoo.com

Introduction

Many techniques were recorded in bioinformatics for DNA microarray data. These are mainly based on fold-change analysis, clustering, classification, genetic network analysis, and simulation [1].

The pyrimidines and purines are of great importance [2], where in our laboratory, numerous papers have been published from the structural and coordination chemistry views [3-20].

The pyrimidine nucleus is embedded in a large number of alkaloids, drugs, antibiotics, agrochemicals, and antimicrobial agents. Many fused pyrimidines such as purines and pteridines are biologically active by themselves, or are essential components of very important naturally occurring substances (*i.e.*, nucleic acids).

The manifestation of the purine system in natural products has been reviewed [21]. Fluorouracil or the human immunodeficiency virus (HIV) drug zidovudine compounds are of biological interest in chemotherapy. Ultrashort-acting barbiturates such as thiopental sodium (Pentothal) [22] are often used as general anesthetics, whereas methylphenobarbital [23] is used as antiepilepticum. Some diaminopyrimidines, such as pyrimethamine or trimethoprimare powerful antimalaria drugs used in combination with sulfonamides, is also a potent antibacteriostaticum, whereas minoxidil [24] is used as antihypertensive. Sulfadiazine is one of the chemotherapeutics containing a pyrimidine moiety.

The aim of the present article is related to study themode of bonding, electronic absorption, magnetic properties, thermal analysis (DSC), dielectric constant, electrical conductivity and molecular modeling of barbituric acid, uracil and their Th complexes.

Experimental

The ligands used are

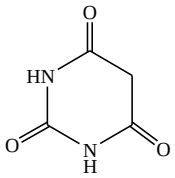

Barbituric acid (BA)

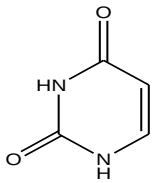

Uracil (U)

Synthesis of metal complexes in the solid state

These were prepared by mixing metal salt solutions with ligand solutions; hence they were refluxed, filtered and dried for the separated products.

The complexes were digested by aqua-regia several times to complete decomposition for the organic ligand compounds. The metal was determined by atomic absorption techniques and complexometric titrations by using published procedures. The analyzed complex is given in Table (1).

Table 1: C, H, N, M elemental analysis for $Th(BA)_2$ complex

Complex	**Colour**	**Formula**	**Calculated/(Found) %**			
			C	**H**	**N**	**M**
$Th(BA)_2$	yellow	$C_{12}H_8N_6O_9Th$	23.54 (23.72)	1.32 (1.55)	13.73 (14.00)	37.90 (38.00)

i. Infrared spectrophotometer: The spectra were recorded using SHIMADZU FTIR spectrophotometer, Central lab, Faculty of Science, Alexandria University.

ii. UV-vis spectrophotometer and molar magnetic susceptibilities

The nujol mull electronic absorption spectra of complexes were recorded using Halios α instrument. Molar magnetic susceptibilities, corrected for diamagnetism using Pascal's constants, were determined at room temperature (298°K) using Faraday's method. The apparatus was calibrated with $Hg[Co(SCN)_4]$.

iii. Thermal analysis

The samples were measured using (DSC-60A detector, aluminum cell, nitrogen atmosphere and 50 ml/min flow rate).

iv. Dielectric and electrical conductivity measurements

1- Four test parameters including impedance $|Z|$, phase angle θ, parallel equivalent static capacitance Cp and loss tangent tan δ were measured for complexes in the solid state at constant voltage 0.80 volt but different temperatures (40-240°C) and at variable frequencies (500 Hz - 5 MHz) using HIOKI "3532-50 LCR HITESTER" instrument.

2- The complexes were prepared in the form of tablets at a pressure of 6-7 tons/cm^2 with 10 mm diameter and 1.48 mm thickness. Silver metal was evaporized on the major faces of each test piece to improve the contact with the measuring electrodes. The tablets were hold between two copper electrodes and then inserted with the holder vertically into cylindrical electric furnace. The potential drop across the heater was varied gradually through variable transformer to produce slow rate of increasing the temperature to get accurate temperature measurements using a pre-calibrated Cu-constantan thermocouple attached to the sample.

3- The dielectric constant ε, the dielectric loss ε″, real part of impedance Z′, imaginary part Z″, the conductivities $\sigma_{a.c.}$ (a.c.: alternating current condition), the relaxation times τ_o, τ and the activation energies ΔE of the complexes were calculated.

v. Molecular Modeling

The ChemOffice Ultra 2004 computer and HyberChem programs are used for molecular modeling studies of the ligands and their complexes.

Results and Discussion

Mode of bonding of barbituric acid (BA) and its Th complex

The data are given in Table (2):

Table 2: Fundamental infrared band (cm^{-1}) of barbituric acid, uracil and their Th complex. (sp: splitted)

Barbituric acid (BA)	$Th(BA)_2$	Uracil	Th-U	Assignments
3552	3360(sh)	3410	3418	υ_{OH}
3478	-			
3182	3177	3111	3101	
{3096}sp	{3123}sp	3041	3042	υ_{NH}
-	3003			
2876	2926	-	-	υ_{CH}
2830	2827			
1744	1710	1740	1724	
{1718}sp	-	1714	-	$\upsilon_{C=O}$
1617	1634	1666	-	$\upsilon_{C=N}$
-	1603	1643	1643	
1526	-	1522	1512	$\upsilon_{C=C}$
1410	1464	1460	1454	δ_{NH}
1366	1385	1420	1412	υ_{C-O} , δ_{CH}
1349	1346	1389	-	
1285	1288	-	-	υ_{C-O} ,δ_{OH}
1232	1209	1244	1231	υ_{C-N}
1193	-			
-	1084			υ_{C-O} , υ_{C-N}
1028	1003	1000	997	υ_{C-C}
936				
733	827	856	856	
739	777	822	-	
656	692	756	764	ρ_{CH} , ρ_{OH}
632	681			
-	538	-	546	υ_{M-O}
-	384	-	430	υ_{M-N}

a- BA gave four IR bands [25] at 3552, 3478, 3182 and 3096 cm^{-1} due to υ_{OH} and υ_{NH}. The lower frequency of the υ_{NH} band compared to its normal position (3460-3400 cm^{-1}) points to the presence of an intramolecular hydrogen bonds of the type OH---N [26].

b- Shifts of the υ_{OH} band of the free ligand occured upon complexation, Table (2), due to the existence of coordinated water moleculesor M–O and hydrogen bond formations [27].

c- The band at 2876 cm^{-1} in the free ligand is due to υ_{CH} .

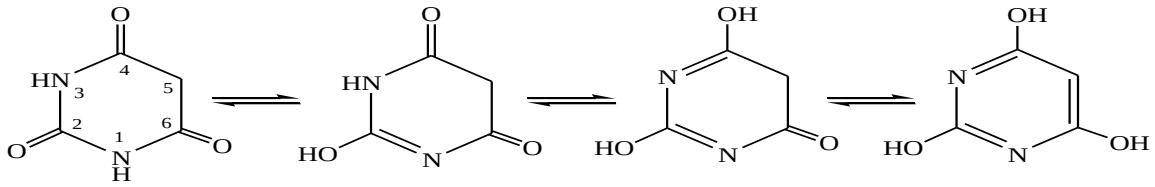

(sp (II) (III) (IV)

d- The shifts or disappearance of both the υ_{NH} and $\upsilon_{C=O}$ bands, Table (2), suggest that these groups are strongly involved in the structural chemistry of the complexes. This is supported either by the probable existence of M–N bands or the free ligand may be subjected to half keto-half enoltautomerism and equlibria in the solid state [15], i.e. conversion of –CNH to C=N occurred.

Structure (IV) represents BA as 2,4,6-trihydroxypyrimidine. X-ray analysis indicated that structure (I) is the predominant form in the solid state [15].

e- New IR bands of the complex appeared at (503-536 cm^{-1}) and (343-417 cm^{-1}) assigned as υ_{M-O} and υ_{M-N}, respectively. The υ_{OH}, υ_{C-N} and υ_{C-O} bands of BA are shifted on complexation, indicating M–O interaction.

f- BA is of bidentate or tridentate bonding. The bidentate chelation is suggested to be through N(1) and C(2)O while the tridentate interaction is via C(2)O, N(3) and C(4)O.

For $Th(BA)_2$ complex, barbituric acid is tautomerized to give tridentate centers for coordination [3] and the presence of (υ_{OH} at 3360 cm^{-1}, υ_{NH} band at 3177-3123 cm^{-1}) upon complexation of $Th(BA)_2$, give a probability of association through hydrogen bonding. The following geometry is proposed:

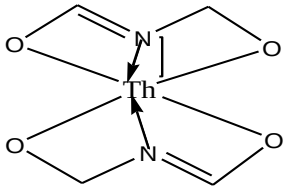

Studies on uracil (U) and its Th complex, Table (2).

The bands at 3410 cm^{-1} and 3418 cm^{-1} in uracil and its Th complex, respectively, are due to υ_{OH} of type N-H…O [12,13].

The uracil υ_{NH} band at 3111 cm^{-1} is strongly affected on complexation with Th by shifting to lower wave number 3101 cm^{-1} which gives indication for Th-N interaction [10,14].

Both $\upsilon_{C=O}$ bands of uracil at 1740 and 1714 cm^{-1} are affected on complexation to Th with different degrees. The first band is at 1724 cm^{-1} and the second band is absent, to assign the presence of Th-O interaction [13].

The $\upsilon_{C=N}$ bands of uracil at 1666 and 1643 cm^{-1} are assigned and compared upon complexation. The first band is absent while the second band isn't affected. Thus, uracil acts as a tridentate ligand through oxygen and nitrogen atoms on reaction with Th [11,14].

From data collected in Table(2) for $Th(U)_2$ complex, the presence of υ_{OH}, υ_{NH} and $\upsilon_{C=O}$ bands at 3418 cm^{-1}, 3101-3042 cm^{-1} and 1724 cm^{-1}, respectively, upon complexation give a probability of association through hydrogen bonding.

The $Th(BA)_2$ complex gave electronic spectral bands at 311, 325 nm with μ_{eff} = 3.32 B.M, assigned to π-π* and d-d electronic transitions and typified the existence of octahedral high spin states [17].

Thermal analysis

The thermal behavior of $Th(BA)_2$ complex has been studied applying differential scanning calorimetry (DSC) [28-31], Figure (1),Table (3).

Table 3: DSC data and thermodynamic paramerters of $Th(BA)_2$ complex

Compound	Heat range °C	T_m °C	ΔH J/g	ΔS J/g.°C	a	b	α	γ
$Th(BA)_2$	264.96 – 321.27	301.93	-47.07	-0.156	-0.077	15.919	-2×10^{-8}	-0.036
	323.62 – 424.85	397.48	-100.75	-0.253	-0.467	211.375	-5×10^{-7}	0.083
					-0.818	411.120	-1×10^{-6}	-0.279
					1.134	-718.675	2×10^{-6}	-0.861
					-0.897	512.346	-8×10^{-7}	0.243
					0.800	-634.178	1×10^{-6}	-0.574
					0.139	-170.955	2×10^{-8}	-0.111
					-0.633	393.655	-4×10^{-7}	0.114

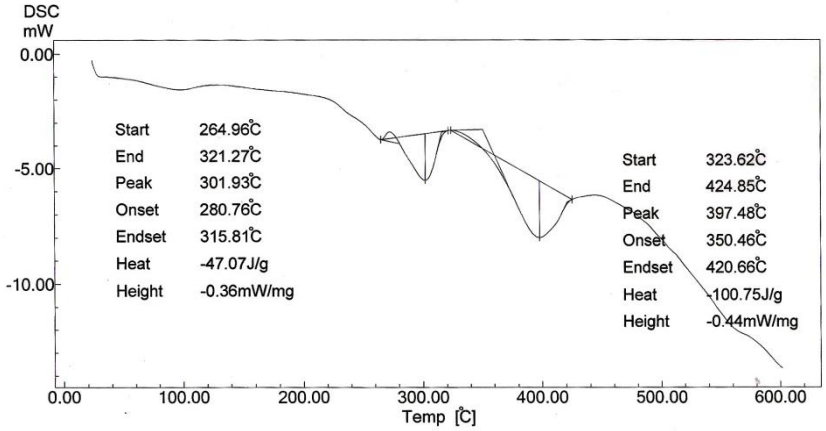

Figure 1: DSC for $Th(BA)_2$

The Debye model [32] is used to describe capacity change over a large temperature range and C_p can be represented by the following empirical form: $C_p = aT + b$.

By plotting C_p versus T, a straight line is obtained, where a and b are parameters which can be determined from the slope and intercept of the line, respectively, Figure (2), Table (3).

The applications based on Debye model for selected complexes are given from the following equations [33]:

$$C_p \simeq C_v = \alpha T^3 + \gamma T , \qquad \frac{Cp}{T} = \alpha T = \alpha T^2 + \gamma$$

where α and γ are the coefficients of the lattice and electronic heat capacities, respectively. C_v is the heat capacity at constant volume which is assumed to be equal to C_p.

The relationships of $\frac{Cp}{T}$ versus T^2 gives straight line with slope α and interceptγ, Figure (3), Table (3).The straight lines are analyzed and the validity is calculated with R^2 values for each line, Figures(2, 3).

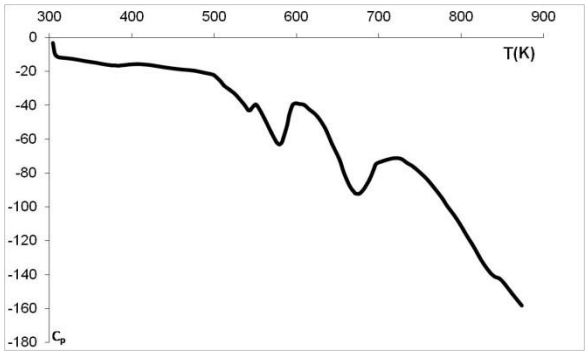

Figure 2: Cp –T relationship for Th(BA)$_2$

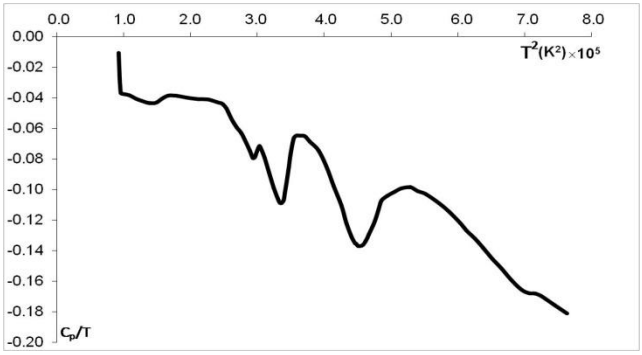

Figure 3: $\frac{Cp}{T}$ –T^2 relationship for Th(BA)$_2$

The change in enthalpy (ΔH) for any phase transformation [34] taking place at any peak temperature, T_m, can be given by the following equation:

$$\Delta S = \frac{\Delta H}{T_m} \qquad \text{(at equilibrium, } \Delta G = 0)$$

The values of T_m(the peak temperature at which the peak is maximum or minimum), ΔH, ΔS, (a, b) parameters of Debye model, α and γ are given in Table (3).

The Th(BA)$_2$ complex gave exothermic peaks. All the change of entropy values, ΔS have –ve signs where the activated transition states are more ordered, i.e. in a less random molecular configuration than that the reacting complexes [28,31].

Dielectric measurements

The dielectric parameters for the investigated complex are illustrated in terms of temperature and frequency (ln f) changes, Figure (4). The more spotlight points, could be given as follows:

1- For a parallel-plate condenser in which a dielectric tablet fills the space between the plates, the capacitance is given by[35]: $C_P = A\varepsilon\varepsilon_o / d$

Where ε_o is the permittivity of a vacuum and its value is approximately 8.854×10^{-12} F m^{-1}, ε is the dielectric constant of a dielectric, a and d are the area and the thickness of the matter tablet, respectively. The capacitance (C_P) decreases with increasing the applied frequency in some different ranges which may be attributed to the effect of charge redistribution by carrier hopping on defects [36]. At low frequency, the charge on defects can be rapidly redistributed so that defects closer to the positive side of the applied field become negatively charged, while defects closer to the negative side of the applied field become positively charged. This leads to screening of the field and an overall reduction in the electric field. Because capacitance is inversely proportional to the field, this reduction in the field for a given voltage results in the increased capacitance observed as the frequency is lowered. In case of high frequency, the defects no longer have enough time to rearrange in response to the applied voltage, hence the capacitance decreases.

2- The complex dielectric permittivity, $\varepsilon^*(\omega)$ is given as follows [37]: $\varepsilon^*(\omega) = \varepsilon'(\omega) - i\varepsilon''(\omega)$

where $\varepsilon'(\omega)$ and $\varepsilon''(\omega)$ are the real and imaginary parts of the complex permittivity, respectively. ωis the angular frequency, $\omega = 2\pi f$ and $i = \sqrt{-1}$.

$\varepsilon'(\omega) = \varepsilon \sin\theta$, $\varepsilon''(\omega) = \varepsilon \cos\theta$ where θ is the phase shift.

ε′ and ε″ decrease with increasing frequency (ln f), which can be explained as follows:

(a) At low frequencies the dielectric constant for polar materials is due to the contribution of multi-component of polarizability, deformational polarization (electronic and ionic polarization) and relaxation polarization (orientational and interfacial polarization) [38].

(b) When the frequency begins to increase, the dipoles will no longer be able to rotate sufficiently rapidly, so that their oscillations begin to lag behind those of the field. As the frequency is further increased, the dipole will be completely unable to follow the field and the orientation polarization stopped, so ε′ and ε″ decrease at higher frequencies approaching a constant value due to the interfacial or space charge polarization only [39].

3- The relative permittivity and dielectric loss values for the complexes, Figure (4), reveal semiconducting features based mainly on the hopping mechanism [40].

4- The loss tangent, tan $\delta = \varepsilon''/\varepsilon'$, $\delta = 90° - \theta$ which is decreased with increasing frequency.

5- The real and imaginary parts of the complex impedance are given by: $Z' = Z \cos \theta$, $Z'' = Z \sin \theta$where Z′ and Z″ are the real and imaginary parts of the impedance, respectively.

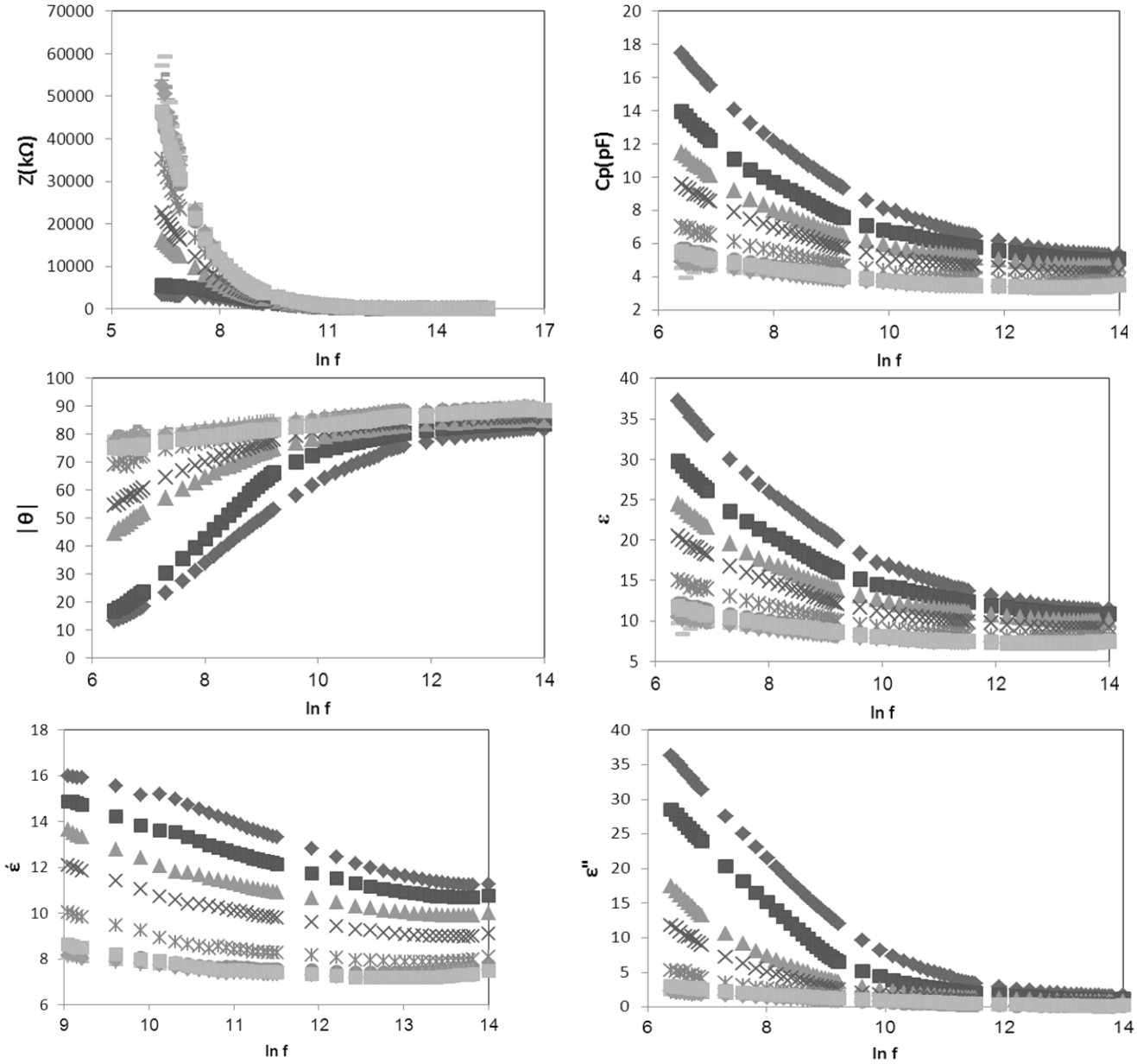

Figure 4: The dielectric parameters (Z, C_P, $|\theta|$, ε, ε′, ε″, tan δ) - ln f relationships for $Th(U)_2$ at different temperatures ◆ 40°C,■ 60°C, ▲80°C, ×100°C, ✱120°C,●140°C,+ 160°C,▬180°C,— 200°C,◆220°C and■240°C

The impedance (Z) is mostly decreased with increasing frequency, Figure (4). The Z″-Z′ relationships are illustrated in Figure (5) at different temperatures. Dispersion arising during the transition from full orientational polarization at zero or low frequencies to negligible orientational polarization at high radio frequencies is referred to as dielectric relaxation [41]. The rate of decay and build-up of the orientational polarization, as given by the relaxation time τ, will depend upon the thermal energy of the dipoles as well as upon the internal or molecular friction forces encountered by the rotating dipoles.

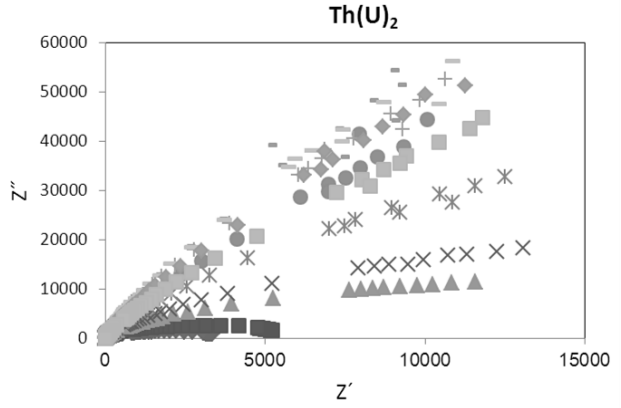

Figure 5: Z″-Z′ relationship for complexes at different temperatures ◆40°C,■60°C, ▲80°C,×100°C, ✱120°C,● 140°C, + 160°C,▬180°C,▬200°C,◆220°C and■240°C

The most used of these methods consists by plotting the imaginary part ε″(ω) for a certain frequency against the real part ε′(ω) at the same frequency [42]. This diagram may be called the complex locus diagram or Argand diagram and was applied to dielectrics by Cole and Cole [43].

Cole and Cole generalized the representation of a Debye dielectric by a circular arc plot in the complex plane so that it is applied to a certain type of distributions of relaxation times, so

$$v/u = (\omega\tau_o)^{1-\alpha}$$

where ω is the angular frequency. The parameter α equals zero when the compound has only one relaxation time, whereas for a series of relaxation times, the value of α varies between 0 and 1. The extent of the distribution of relaxation times increases with increasing parameter α. On the other hand, the value of τ_o decreases with increasing temperature. The molecular relaxation time τ could be determined based on the following equation [43]:

$$\tau = \frac{2\varepsilon_s + \varepsilon_\infty}{3\varepsilon_s}\tau_o$$

The relaxation time is interpreted as the average time which a molecule spends in one of the equilibrium positions before jumping to the other one. The temperature dependence of τ can be expressed for thermally activated processes as [38]:

$$\tau = \tau_o e^{E_o/kT}$$

where τ_o is a constant characteristic relaxation time and represents the time of a single oscillation of a dipole in a potential well, E_o is the energy of activation for the relaxation of the dipole, k is the Boltzmann constant and τ represents the average or most probable value of the spread of the relaxation times. The Cole-Cole diagrams for $Th(U)_2$ complex at different temperatures, Figures (6), Table (4) reveal mainly non-Debye type.

The variation of lnτ as a function of reciprocal absolute temperature for ligands and complexes, Figure (7), assigned that as the temperature increases, the relaxation time for each relaxator becomes smaller. The activation energy for the relaxation process of $Th(BA)_2$ complex is 6.16kJ mol^{-1}.

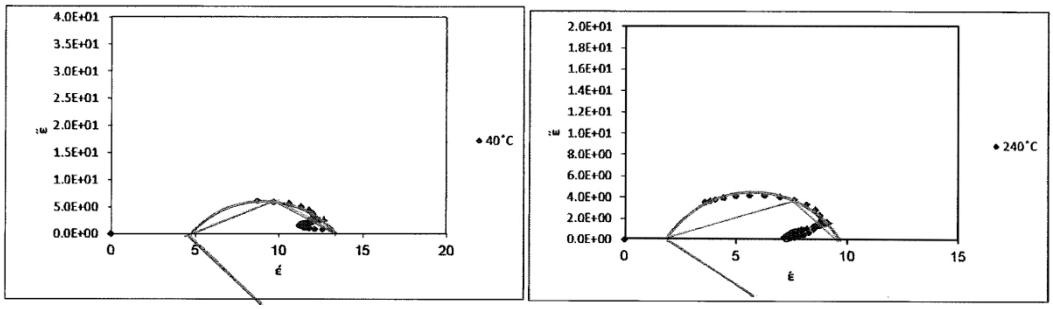

Figure 6: Cole-Cole diagrams for $Th(U)_2$ at different temperatures

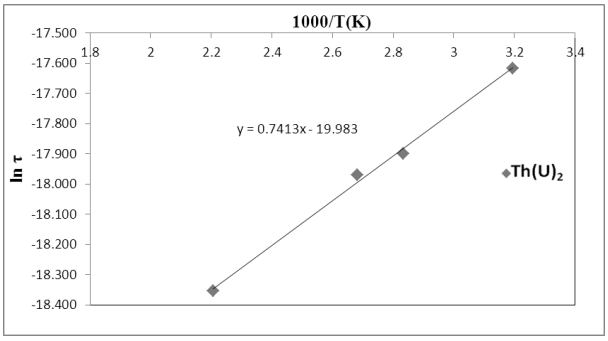

Figure 7: ln τ-1000/T relationship for $Th(U)_2$ complex

Table 4: The dielectric data obtained from the analysis of Cole-Cole diagrams for $Th(U)_2$ complex

Compound	Temperature (K)	ω	V	u	α	$\frac{\pi}{2}$	α	1 - α	$\tau_0 \times 10^{-8}$	ε_s	ε_∞	$\tau \times 10^{-8}$	ln τ
	313		0.90	1.15	45	0.5000	0.5000	2.86702	13.41	4.55	2.23560	-17.6162	
	333		1.00	1.80	45	0.5000	0.5000	1.44476	13.64	1.82	1.02743	-18.3936	
	353		1.05	1.75	23	0.2556	0.7444	2.35687	12.73	1.82	1.68357	-17.8998	
	373		0.90	1.60	22	0.2444	0.7556	2.18585	11.59	1.82	1.57165	-17.9686	
	393		0.80	1.70	30	0.3333	0.6667	1.51113	10.34	2.07	1.10826	-18.3179	
$Th(U)_2$	413	21362830.0	0.80	1.75	32	0.3556	0.6444	1.38943	10.00	2.07	1.02215	-18.3988	
	433		0.80	1.70	32	0.3556	0.6444	1.45335	10.00	2.07	1.06918	-18.3538	
	453		0.80	1.70	32	0.3556	0.6444	1.45335	10.00	2.07	1.06918	-18.3538	
	473		0.80	1.70	31	0.3444	0.6556	1.48245	10.00	1.90	1.08219	-18.3417	
	493		0.80	1.70	31.5	0.3500	0.6500	1.46795	9.82	1.90	1.07331	-18.3499	
	513		0.80	1.70	32	0.3556	0.6444	1.45335	9.66	1.90	1.06419	-18.3585	

τ Ranges for $Th(U)_2$ is (1.22353×10^{-8}- 5.25957×10^{-6}).

Electrical conductivity measurements

The alternating current conductivity (σ) is calculated according to the following equation:

$$\sigma\ (\Omega^{-1}\ cm^{-1}) = \omega \times C_P\ (pF) \times \tan\delta \times \frac{d}{A}\ (cm^{-1}) \times 10^{-12}$$

The frequency dependence of a. c. conductivity for $Th(U)_2$ complex at different temperatures, Figure (8), where the a. c. conductivity gradually increases with increasing the frequency. At lower frequencies the grain boundaries are more effective than grains in electrical conduction hence the hopping of ions are bound at lower frequencies. As the frequency of the applied field increases the conductive grains become more active and promote the conduction mechanism [44].

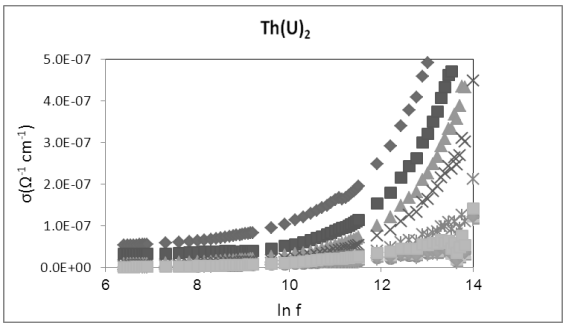

Figure 8: A. C. conductivity σ-ln f relationship for $Th(U)_2$ complexes at different temperatures ◆40°C, ■60°C, ▲80°C, ×100°C, ✱120°C, ●140°C, + 160°C, ▬180°C, ▬200°C, ◆ 220°C and ■ 240°C

The conductivities have a magnitude close to that of semiconductors [45], where the electrons in the orbitals are not of sufficient mobility to be promoted.

The investigation of electron transport in disorder systems has been gradually developed, while forgap states is of particular interest, because of their effect on the electrical properties of semiconductor materials. Several concepts proposed by many workers start from the premise that the contribution of carriers hopping between localized states to electrical conductivity is expected in amorphous semiconductors. The hopping conduction can be easily distinguished from that of the band conduction by measuring the frequency dependence of conductivity, which as expected, is due to conduction in localized states.

The electrical conduction mechanism of solids is based on [46,47]:

1- The conductivity depends on the mobility of π-electrons.
2- In the molecule, the π-electrons are localized in the molecule framework and their delocalization requires activation energy.
3- The delocalized π-electrons migrate to the neighboring molecule by tunnel effect. As the temperature increases, the bonds are exhausted resulting in an increase of the conductivity.

The electrical conductivity of substances at a given frequency varies exponentially with the absolute temperature according to the Arrhenius relation:

$$\sigma = \sigma_o \, e^{-\Delta E/kT}$$

where σ is the electrical conductivity at an absolute temperature T, σ_o is the pre-exponential factor, ΔE is the activation energy. The activation energy data and $\ln\sigma_o$ values for ligands and complexes are given in Figure (9) and Table (5).

Table 5: The activation energy data ΔE(kJ mol^{-1}) and ln σ_o values for $Th(U)_2$ complex at different frequencies

Compound	Frequency (kHz)	ln σ_o	ΔE (kJ mol^{-1})
$Th(U)_2$	10	-14.15	20.08
	50	-12.41	23.11
	100	-10.07	31.91
	500	-11.05	24.26
	1000	-9.90	29.56

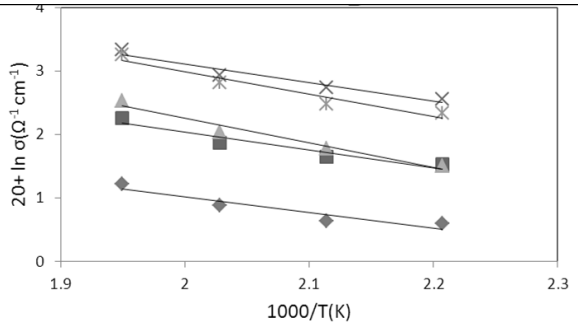

Figure 9: ln σ-1000/T relationship for Th(U)$_2$complex at different frequencies ◆10kHz,■50 kHz, ▲100 kHz,✕500 kHz and ✕1000 kHz

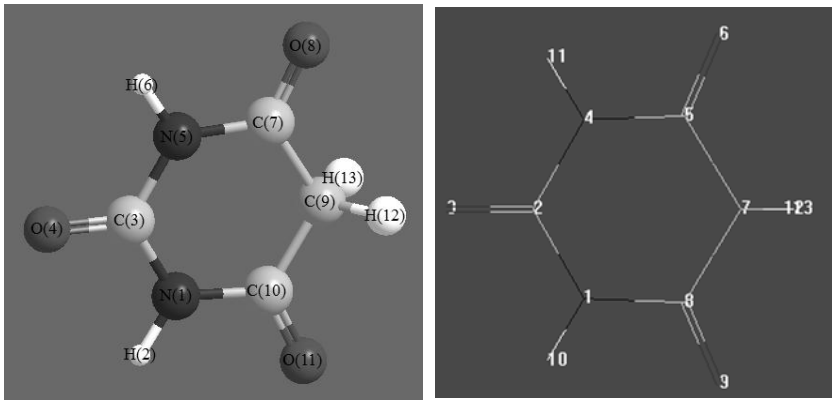

Figure 10: The molecular modeling of Barbituric acid (BA), a) ChemOffice, b) HyperChem

The relationship between molecular structure and electrical properties was deduced, where two pathways for the conduction of electricity may be expected. The first conducting process occurring in the lower temperature region is attributed to n→π* transitions which require less energy to be performed. In the upper temperature region, conduction could be attributed to π→π* transitions which need more energy to participate in electronic conduction. The observed increment of conduction in the upper temperature region may be attributed to interactions between n→π* and π→π* transitions. The lower temperature range is the region of extrinsic semiconductor where the conduction is due to the excitation of carriers from donor localized level to the conduction band. In the upper temperature range, the intrinsic region is reached where carriers are thermally activated from the valence band to the conduction band. This behavior can be explained as follows: the upper temperature range may be attributed to the interaction between the electrons of d-orbitals and the p-orbitals of the ligand. This interaction will lead to small delocalization of the p-electronic charge on the ligand which tends to increase the activation energy. The presence of d-electrons in a narrow energy band leads to magnetic ordering and degeneracy of d-bands with respect to the orbital quantum number, which is only partially lifted in a crystal field [48].

For Th(U)$_2$ complex during thermal agitation, an additional increase in electrical conductivity occurs, which probably indicating a discontinuity of the chemical bonds existing in the structure.

Th forms a bridge with the ligands, thus facilitating the transfer of current carriers with some degree of delocalization in the excited state during measurements. Meanwhile, this leads to an increase of the electrical conductivity with a decrease in energy of activation [48].

Molecular Modeling

The molecular modeling calculations of the compounds, Figure (10) are given concerning the bond lengths, bond angles, dihedral angles and HyberChem data, Table (6b). These calculations are based on using molecular orbital package (MOPAC) for minimizing energies where the Austin Model 1(AM1) method is used, also Parameterized Model 3(PM3) is applied for HyberChem.

Different parameters (heat of formation, gradient norm, dipole, charges, solvation in water, electrostatic potential, molecular surfaces, spin density, hyperfine coupling constants and polarizabilities) are of major importance to control the modeling of the compounds.

Table 6a: Quantum chemical parameters (eV) of compounds calculated by PM3 method

Compound	E_{HOMO}	E_{LUMO}	$\Delta E=(E_L-E_H)$	χ	μ	η	σ	ω
BA	-10.828	-0.421	10.407	5.6245	-5.6245	5.2035	0.1922	3.0398
U	-9.710	-0.511	9.199	5.1105	-5.1105	4.5995	0.2174	2.8391

Table (6b): HyperChem calculations of compounds calculated by PM3 method

HyperChem calculations	(kcal/mol) (BA)	(kcal/mol) (U)
Total energy	-40174.049	-33385.590
Binding energy	-1420.823	-1304.879
Isolated atomic energy	-38753.226	-32080.711
Electronic energy	-165585.243	-132951.621
Core-core interaction	125411.193	99566.030
Heat of formation	-124.178	-67.794
Dipole moment	0.810 Debye.	3.990 Debye.
Net charges of atoms	(1(-0.024), 2 (0.230), 3(-0.361), 4(-0.024), 5(0.251), 6(-0.334), 7(-0.145), 8(0.251), 9(-0.334), 10(0.127), 11(0.127), 12 (0.117) and 13(0.118)).	(1(-0.011), 2 (0.208), 3(-0.387), 4(0.089), 5(-0.065), 6(-0.277), 7(0.298), 8(-0.352), 9(0.121), 10(0.105), 11(0.124) and 12(0.145)).

Quantum chemical parameters such as the highest occupied molecular orbital energy (E_{HOMO}) and the lowest unoccupied molecular orbital energy (E_{LUMO}) were given using HyberChem modeling, where energy gap (ΔE) and parameters which give information about the reactive chemical behavior of compounds such as electronegativity (χ), chemical potential (μ), global hardness (η), softness (σ) and electrophilicity index (ω) were calculated, Table (6a).

$$\Delta E = E_{LUMO} - E_{HOMO}$$

The concepts of these parameters are related to each other, the energies of the (HOMO) and (LUMO) orbitals of the molecule are related to ionization potential (I) and the electron affinity (A), respectively, and their relations with χ and μ are given by the following equations:

$$I = -E_{HOMO} \qquad \mu = -\chi$$

$$A = -E_{LUMO} \qquad \mu = \frac{-(I+A)}{2} = \frac{E_{HOMO} + E_{LUMO}}{2}$$

The qualitative definition of hardness is related to the polarizability, because a decrease of the energy gap usually leads to an easier polarization of the molecule.

$$\eta = \frac{I-A}{2} = \frac{E_{LUMO} - E_{HOMO}}{2}$$

The inverse of the hardness is equal to softness, (σ) as follows:

$$\sigma = \frac{1}{\eta}$$

The energy difference between the HOMO and LUMO (HOMO-LUMO gap) can be used to predict the strength and stability of transition metal complexes. Hard molecules have a large HOMO-LUMO gap while, soft molecules have a small HOMO-LUMO gap. Soft molecules have small excitation energies to the excited states; therefore they will be more polarizable and more reactive than the hard molecules. Hard molecules resist changes in their electron number and distribution.

The electrophilicity index (ω) in terms of chemical potential (μ) and hardness (η) is given from the equation [49]:

$$\omega = \frac{\mu^2}{2\eta}$$

HOMO-LUMO gaps are mostly decreased and softness increased upon complexation with different ligands, also the total evolved energies are increased which give stabilization for complex formation.

References

[1]. Integrated bioinformatics analysis to identify 15 hub genes in breast cancer, H. Jin, X. Huang, K. Shao, G. Li, J. Wang, H. Yang and Y. Hou, OncologyLetters, 1023-1034 (2019).doi.org/10.3892/ol.2019.10411

[2]. Modification of Purine and Pyrimidine Nucleosides by Direct C-H Bond Activation, Y. Liang and S.F. Wnuk, Molecules, 20(3), 4874-4901(2015).

[3]. Synthesis and Characterization of New Azopyrimidine Complexes, M.S. Masoud, A. Soayed, A.E. Ali and O.K. Sharsherh, J. Coord. Chem., 56(8):725-742(2003).

[4]. Synthesis, Spectral, Computational and Thermal Analysis Studies of Metallocefotaxime Antibiotics, M.S. Masoud, A.E. Ali, G.S. El-Asala, Spectrochim. Acta Part A: Molecular and Biomolecular Spectroscopy, 149, 363-377 (2015).

[5]. Synthesis, Spectral, Computational and Thermal Analysis Studies of Metalloceftriaxone Antibiotic, M.S. Masoud, A.E. Ali, G.S. El-Asala, J. of Molecular Structure, 1084, 259-273 (2015).

[6]. Structural, Spectral and Thermal Analysis of Some Metallocephradines, M.S. Masoud, A.E. Ali, D.A. Ghareeb, N.M. Nasr, Journal of Molecular Structure, 1099, 359-372 (2015).

[7]. Synthesis, Molecular Spectroscopy and Thermal Analysis of some Cefepime Complexes, M.S. Masoud, A.E. Ali, D.A. Ghareeb, N.M. Nasr, J. of Molecular Structure, 1107, 189-201 (2016).

[8]. Synthesis, Spectral Characterization and Thermal Analysis of Some Alloxan, Carmine, Naphthol Yellow S and Hematoxylin Complexes, M.S. Masoud, R.H. Mohamed, A.E. Ali and N.O. EL-Ziani, J. Chemical and Pharmaceutical Research, 8 (1), 639-662 (2016).

[9]. Complexing Properties of Some Pyrimidines, M.S. Masoud, E.A. Khalil and S.S. Haggag, Nucleosides, Nucleotides and Nucleic Acids 25(1), 73-87 (2006).

[10]. Structural chemistry and thermal properties of some pyrimidine complexes, M.S. Masoud, S.A. Abou El-Enein and H.M. Kamel, Ind. J. Chem., 41A, 297-303 (2002).

[11]. Spectral properties of some metal complexes derived from uracil, thiouracil and citrazinic acid compounds,M.S. Masoud, E.A. Khalil, A.A. Ibrahim and A. El-Marghany, Spectrochim. Acta 67A, 662-668 (2007).

[12]. Electronic spectral properties of some substituted arylazothio barbiturate compounds in presence of different solvents,M.S. Masoud, S.A. Abou El-Enein and N.A. Obeid, Z. für Phys. Chem., 215, 7, 867-881 (2001).

[13]. Dissociation constants of substituted arylazo babituric and thio barbituric acids,M.S. Masoud, A.K. Ghonaium, R.H. Ahmed, A. A. Mahmoud and A.E. Ali, Z. für Phys. Chem., 215, 4, 531-542 (2001).

[14]. Ligating properties of 5-nitrobarbituric acid,M.S. Masoud, A.K. Ghonaim, R.H. Ahmed S.A. Abou El-Enein and A.A. Mohmoud, J. Coord. Chem., 55(1), 79-105 (2002).

[15]. Synthesis and characeterization of new azopyrimidine complexes, M.S. Masoud, A.A. Soayed, A.E. Ali and O.K. Sharsherah, J. Coord. Chem., 56(8), 725-742 (2003).

[16]. Studies on Transition Metal Murexide Complexes,M.S. Masoud, T.S. Kasem, M.A. Shaker and A.A. Ali, J. Therm. Anal. Calorim., 84(3), 549-555 (2006).

[17]. Synthesis and Charecterization of some Pyrimidine, Purine, Amino Acid and Mixed Ligand Complexes, M.S. Masoud, M.F. Amira, A.M. Ramadan and Gh.M. El Ashry, Spectrochim.Acta, 69A, 230-238 (2008).

[18]. Thermal properties of some biologically active 5-(p-substituted phenylazo)-6-aminouracil complexes,M.S. Masoud, S.A. Abou El-Enein and A.M. Ramadan and A.S. Goher, J. Anal. Appl. pyrolysis, 81(1), 45-51 (2008).

[19]. Thermal Studies of Some Purine Compounds and Their Metal Complexes,M.S. Masoud, A. El-Merghany, A.M. Ramadan and M.Y. Abd El-Kaway, J. Therm. Anal. Calorim., 101(3), 839-847 (2010).

[20]. Synthesis, computational, spectroscopic, thermal and antimicrobial activity studies on some metal-urate complexes,M.S. Masoud, M.A. Shaker, A.E. Ali and G.S. El-Asala, Spectrochim. Acta, 90A, 93-108 (2012).

[21]. The chemodiversity of purine as a constituent ofnatural products, H. Rosenmeyer, Chem. Biodiversity, 1, 361-401 (2004).
[22]. In vivo and in vitro effects of different anaesthetics on platelet function, P.L. Dordoni, L. Frassanito, M.F. Bruno, R. Proirtti, R. De Cristofaro, G. Ciabattoni, G. Ardito, R. Crocchiolo, R. Landolfi and B. Rocca, Br. J. Haematol, 125, 79-82 (2004).
[23]. M. J. Eadie and W. D. Hooper, "Other Barbiturate-Methylphenobarbital", In "Antiepileptic Drugs", Eds. E.H. Levy, R. Mattson, B.S. Meldrum, E. Perucca, Lippincott-Williams and Wilkins, Philadelphia (2002).
[24]. The psychosocial consequences of androgenetic alopecia: a review of the research literature, T.F. Cash, Br. J. Dermatol., 141 (3), 398-405 (1999).
[25]. Spectral, Magnetic and Thermal Properties of Some Thiazolylazo Complexes,M.S. Masoud, G.B. Mohamed, Y.H. Abdul-Razek, A.E. Ali and F.N. Khairy, J. Kor. Chem. Soc., 46(2), 99-116 (2002); Studies on Some Thiazolylazo Compounds and Their Cobalt, Nickel and Copper Complexes,Spectrosc. Lett., 35, 377-413 (2002).
[26]. S. Pati, "The Chemistry of the Hydrazo, Azo and Azoxy Groups", Part 1, Wiley, New York (1975).
[27]. Synthesis and characterization of amino alcohol complexes,M.S. Masoud, S.A. Abou El-Enein, I.M. Abed and A.E. Ali, J. Coord. Chem. 55(2), 153-178 (2002).
[28]. Thermal and electrical behaviour of nickel (II) and copper (II) complexes of 4-acetamidophenylazo-p-cresol (4-acetylamino-2-hydroxy-5-methyl azobenzene),M.S. Masoud, E.A. Khalil, E. El-Sayed El-Shereafy and S.A. El-Enein, J. Therm. Anal., 36,1033-1038 (1990).
[29]. Thermal decomposition of monosaccharides derivatives applied in ceramic gelcasting process investigated by the coupled DTA/TG/MS analysis, P. Bednarek and M. Szafran, J. Therm. Anal. Calorim., 109, 773-782 (2012).
[30]. D. Fox, M. M. Labes and A. Weissberger, Phys. and Chem. of the Org. Solid State, Vol. II, Wiley-Interscience, New York(1965).
[31]. Solid-state thermal polymorphic transformation for some solvents of some azo complexes,M.S. Masoud, A.M. Donia and S.A. El-Enein, Thermochim. Acta, 161, 217-222 (1990).
[32]. Specific heat capacity and Debye temperature of zirconia and its solid solution, C. Degueldre, P. Tissot, H. Lartigue and M. Pouchon, Thermochim. Acta, 403, 267-273 (2003).
[33]. Physicochemical studies of the reaction of 99mTc with 5,5′-diethyl barbituric acid, adenine, d-glucose and thiobarbituric acid at different temperatures, M.S. Masoud, M.F. El-Shahat and A.S. El-Kholany, Spectrochim. Acta, 127A, 216-224 (2014) **.**
[34]. Analyse thermique differentielle et cinetique de reaction III. Surface des pics d'analyse thermique differentielle et applications, K. Traore, J. Therm. Anal., 4, 135-145 (1972).
[35]. H.M. Rosenberg, "The Solid State", 3rd Ed., Oxford Univ. Press (1997).
[36]. B. Tareev, "Physics of Dielectric Materials", Mir Publishers, Moscow (1979).
[37]. Dielectric studies of $Cd_{1-x-y}Zn_xMn_yTe$ crystals, H.M. Lin, Y.F. Chen, J.L. Shen and W.C. Chou, J. Appl. Phys., 89, 4476-4479 (2001).
[38]. Dielectric behavior and ac electrical conductivity of nanocrystalline nickel aluminate, S. Kurien, J. Mathew, S.Sebastian, S.N. Potty and K.C. George, Mater .Chem. Phys., 98, 470-476 (2006).
[39]. Prospects in solid state chemistry, J. M. Thomas, Chemistry in Britain, 13 (5), 175-182 (1977).
[40]. A. Zaky and R. Hawley, "Dielectric Solids", Routledge and Kegan Paul Ltd., London, UK (1970).
[41]. H. Fröhlich, "Theory of Dielectrics", Oxford Univ. Press, London (1949).
[42]. V. V. Daniel "Dielectric Relaxation", Academic Press, London and New York (1967).
[43]. Dispersion and Absorption in Dielectrics I: Alternating CurrentCharacteristics,K.S. Cole and R.H. Cole, J. Chem. Phys., 9, 341-351 (1941).
[44]. Dielectric relaxation behavior of $A_xCo_{1-x}Fe_2O_4$ (A = Zn, Mg) mixed ferrites, K. Verma, A. Kumar and D. Varshney, J. Alloys Compd., 526,91-97 (2012).

[45]. Effect of Fast Neutron Irradiation on the Electrical conductivity of Some Azo Pyrazolones at Different Temperatures, M.S. Masoud, A. El-Khatib, M. Kassem and A.R. Youssef, J. Mater. Sci. Lett., 7, 1291-1294 (1988).
[46]. The semiconductivity of organic substances, D. D. Eley and G. D. Parfitt, Trans. Faraday Soc., 51, 1529-1539 (1955).
[47]. Transition to Nonmetallic Behavior in Expanded Liquid and Gaseous Metals, H. Hansel, Ann. Phys., 24 (3), 1947-1951 (1970).
[48]. Thermal and Electrical Behavior of Nickel (II) and Copper (II) Complexes of 4-Acetamidophenylazo-p-Cresol (4-Acetylamino-2-Hydroxy-5-Methyl Azobenzene), M.S. Masoud, E.A. Khalil, E. El-Shereafy and S.A. Abou El-Enein, J. Therm. Anal., 36, 1033-1038 (1990).
[49]. Electrophilicity Index, P. K. Chattaraj and D. R. Roy, Chem. Rev., 107, 46-74 (2007).